

On low eigenvalues of the entanglement Hamiltonian, localization length, and rare regions in disordered interacting one-dimensional systems

Richard Berkovits

Department of Physics, Jack and Pearl Resnick Institute, Bar-Ilan University, Ramat-Gan 52900, Israel

The properties of the low-lying eigenvalues of the entanglement Hamiltonian and their relation to the localization length of a disordered interacting one-dimensional many-particle system is studied. The average of the first entanglement Hamiltonian level spacing is proportional to the ground state localization length and shows the same dependence on the disorder and interaction strength as the localization length. This is the result of the fact that entanglement is limited to distances of order of the localization length. The distribution of the first entanglement level spacing shows a Gaussian-like behavior as expected for level spacings much larger than the disorder broadening. For weakly disordered systems (localization length larger than sample length), the distribution shows an additional peak at low level spacings. This stems from rare regions in some samples which exhibit metallic-like behavior of large entanglement and large particle number fluctuations. These intermediate microemulsion metallic regions embedded in the insulating phase are discussed.

PACS numbers: 73.21.Hb, 71.15.Rn, 71.10.Hf, 71.27.+a

I. INTRODUCTION

Close to 60 years after the concept of localization has been introduced by Anderson¹, the localization transition remains at the center of many current topics, from applications of many body in quantum information² to random lasing³. While for most quantum phases the gap between the ground state energy and the first excited state defines the correlation length, in the localized phase the correlation length corresponds to the localization length, determined by the exponential dependence of the conductance, G , on the linear dimension of the system, L . The localization length, ξ , is defined through the exponential decrease in the conductance in the localized phase $G(L) \sim \exp(-L/\xi)$ ⁴.

Recently, it was realized that ξ should also determine the entanglement properties of a system in the strongly localized regime⁵. One does not expect regions beyond the distance ξ to be entangled. Thus, by dividing a one dimensional system into two regions (see Fig. 1), and studying the entanglement between them, one may hope to gain a measure of ξ through the entanglement properties. Indeed, the averaged entanglement entropy increases logarithmically as long as the length of region A, L_A is smaller than ξ and saturates for $L_A > \xi$ ^{5,6}. Here we would like to use entanglement as a window into the physics of the region within length ξ from the boundary.

The information regarding the entanglement between the regions A and B is encoded in the reduced density matrix (RDM), $\rho_{A(B)}$, of regions A (or B). For a system in a pure state $|\Psi\rangle$, ρ_A is defined as: $\rho_A = \text{Tr}_B |\Psi\rangle\langle\Psi|$, where the degrees of freedom of region B are traced out. It is important to note that diagonalizing ρ_A defines a basis that completely spans the Hilbert space of region A and if there exists any conserved quantum number (for the case discussed in this paper the conserved quantum number is N_A , the number of particles in region A) that

basis is also the eigenvectors of N_A . The eigenvalues of the RDM, $\lambda_i^{N_A}$, are used to extract measures for the entanglement between the regions, such as the entanglement entropy, defined as: $S_A = -\sum_i \lambda_i^{N_A} \ln \lambda_i^{N_A}$, and the Rényi entropy: $S_{nA} = -\frac{1}{1-n} \ln \sum_i (\lambda_i^{N_A})^n$. where the first Rényi entropy ($n \rightarrow 1$) is equal to the entanglement entropy.

Recently Li and Haldane⁷ have suggested a different way to interpret the eigenvalues of the RDM. They noted that the RDM of region A may be seen as a density matrix of a mixed thermal state of an ersatz system described by a Hamiltonian H_A such that $\rho_A = \exp(-\beta H_A)$, where H_A is known as the entanglement Hamiltonian, and $\beta = 1$. Under these conditions the eigenvalues of H_A are given by $\varepsilon_i^{N_A} = -\ln(\lambda_i^{N_A})$. Up until now, these are just mathematical manipulations, but Li and Haldane noted that for a fractional quantum Hall $\nu = 5/2$ state where the edge and the bulk are chosen as the two regions, the eigenvalues $\varepsilon_i^{N_A}$, resembled the true edge excitation spectrum. This is actually quite intuitive since due to geometry, the boundary between regions A and B and the volume of region A are the same, and therefore one should expect H_A to give a reasonable representation of the physics of region A. This suggests that the low-energy entanglement Hamiltonian spectrum shows some correspondence to the true many-body excitations of the partitioned segment (the edge region). This correspondence has been demonstrated for different cases of topological insulators^{8,9}.

The opposite situation is the entanglement between regions A and B for a 1D system depicted in Fig. 1 where the contact between the two regions is a point. As pointed out by Alba et. al.¹⁰, for different 1D gaped systems (i.e., systems with finite correlation length) one expects that the entanglement spectrum will be mainly influenced by a region of order of the correlation length from the boundary. This is similar to the situation in the Anderson localized phase, where there is no gap but the

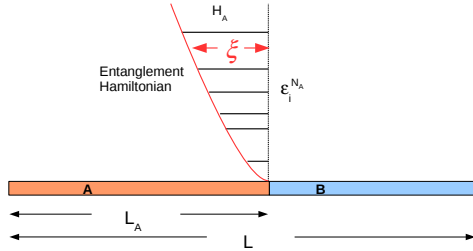


FIG. 1: A schematic representation of the system and the entanglement Hamiltonian H_A . A one-dimensional system of length L is bisected into two regions A and B, with length L_A and $L - L_A$. The reduced density matrix of region A, ρ_A is calculated and its eigenvalues $\lambda_i^{N_A}$ are used to construct the entanglement Hamiltonian H_A and its eigenvalues $\varepsilon_i^{N_A}$. H_A samples the behavior of the system on a scale ξ from the A-B boundary

localization length plays the role of a correlation length⁴. This is highlighted by the saturation of the entanglement entropy once $L_A > \xi$ discussed earlier, as well as by power-law behavior which depends on the localization length of the entanglement spectrum of a highly excited state¹¹ in the many-body localized regime.

In this paper we show that the entanglement spectrum of the ground and low-lying excitation states of a localized interacting 1D many-particle system shows a clear signature of the many-particle localization length. Specifically, the first level spacing of the entanglement energies for a given N_A , $\Delta_1^{N_A} = \varepsilon_2^{N_A} - \varepsilon_1^{N_A}$, is proportional to $1/\sqrt{\xi}$. As we shall explain this is the behavior expected from a many particle state trapped in a potential of width ξ from the boundary. Moreover, the proportionality depends linearly on the strength of particle-particle interactions, U , as expected from charge particles trapped in a potential. It is also shown that deep in the localized regime, where no difference in the localization length between the many-particle ground state and the low-lying states is expected, also $\Delta_1^{N_A}$ is similar. On the other hand, for weaker disorder, where the localization length for low-lying excitations is significantly larger than for the ground state¹², also $\Delta_1^{N_A}$ becomes smaller. The distribution of $\Delta_1^{N_A}$ becomes Gaussian for $\xi \ll L_A$, with a width proportional to disorder and does not depend on U , as might be expected for the level spacing of states in a weakly disordered quantum dot.

This is important not only as a new simple way of determining the localization length of an interacting many-particle system, but mainly as a way to access the properties of disordered many-particle systems on short length scales (of scale ξ) and large energy scales $U/\sqrt{\xi}$. This is

illustrated by using the low lying values of ε to detect and characterize rare regions in the sample which appear for low disorder strongly interacting samples. These regions exhibit metallic-like behavior such as large entanglement and high particle number variance.

The paper is organized as follows: In Sec. II the model for the interacting fermions in a disordered one dimensional system is defined. The next section (Sec. III) discusses the average of the first entanglement level spacing and its relation to the ground state localization length. The following section (Sec. IV) investigates the properties of the distribution of the first entanglement level spacing. The appearance of some rare regions in the sample which exhibit metallic-like features is discussed in Sec. V. The significance of the results and relevance to further work is discussed in Sec. VI.

II. MODEL

In this paper we study spinless electrons confined to a 1D wire of length L with repulsive nearest-neighbor particle-particle interactions and on-site disordered potential, depicted by the Hamiltonian:

$$H = \sum_{j=1}^L \epsilon_j \hat{c}_j^\dagger \hat{c}_j - t \sum_{j=1}^{L-1} (\hat{c}_j^\dagger \hat{c}_{j+1} + h.c.) \quad (1)$$

$$+ U \sum_{j=1}^{L-1} (\hat{c}_j^\dagger \hat{c}_j - \frac{1}{2})(\hat{c}_{j+1}^\dagger \hat{c}_{j+1} - \frac{1}{2}),$$

in which ϵ_j represents the on-site energy drawn from a uniform distribution $[-W/2, W/2]$, \hat{c}_j^\dagger is the creation operator of a spinless particle at site j , and $t = 1$ is the hopping matrix element. The interaction strength is U , with a background positive charge. For this model the localization length $\xi_0 \approx 105/W^{2/3}$ for $U = 0$. The Luttinger parameter is defined as $K(U) = \pi/[2 \cos^{-1}(-U/2)]^{14,15}$, where $K(U = 0) = 1$. As U increases K becomes smaller, and at the transition to a charge density wave ($U = 2$) $K = 1/2$. Renormalization group scaling of the localization length suggests $\xi = (\xi_0)^{1/(3-2K)}$ ^{16,17}, i.e., ξ decreases as the interaction increases and the system becomes more localized.

III. AVERAGED FIRST ENTANGLEMENT LEVEL SPACING

We use the numerical DMRG^{18,19} method to calculate the RDM for the ground state and low-lying excited states of the Hamiltonian depicted in Eq. (1)^{5,12} at half-filling. We calculate the eigenvalues of the RDM for a system of length $L = 700$, different values of disorder $W = 0.3, 0.7, 1.5, 2.5, 3.5, 4, 5$ corresponding to $\xi \sim 1100, 200, 50, 20, 9, 6.5, 4$, different values of interaction strength $U =$

0, 0.3, 0.6, 0.9, 1.2, 1.5, 1.8, 2.1, 2.4 corresponding to $K = 1, 0.91, 0.84, 0.77, 0.71, 0.65, 0.58, 0.49, 0.48$ (the two last values are a continuation of the values K for $U = 2$) and different sizes of region A: usually, $L_A = 10, 20, \dots, L - 10$, for at least 100 realizations of on-site disorder.

Here we concentrate on the first level spacing of the entanglement levels. Since the number of electrons in region A remains a good quantum number of H_A , for each eigenstate of ρ_A one should calculate both λ_i and N_i^A (the number of particles in the region A). Calculating N_i^A does not add to the complexity of the DMRG code²⁰. Thus, the average first level spacing $\Delta_1^{N_A}(L_A) = \langle \varepsilon_2^{N_A}(L_A) - \varepsilon_1^{N_A}(L_A) \rangle$ (where $\langle \dots \rangle$ depicts an average over different realization of disorder) is calculated. It is important to note that if one ignores the subscript N_A and calculates $\varepsilon_2 - \varepsilon_1$ one gets a very different result. Essentially, since eigen-states of ρ_A belonging to different sectors of N_A do not couple, one obtains a spacing of two unrelated energies which does not contain much physical information. On the other hand $\Delta_1^{N_A}$ does not depend strongly on N_A and therefore we also average over values of $N_A \sim L_A/2$ to obtain Δ_1 .

In Fig. 2, $\Delta_1(L_A)$ for different values of disorder W and interaction strength U is presented. Since we expect that there will be no entanglement beyond a region proportional to ξ , the entanglement spectrum should be affected by the shortest length scale of L_A or ξ . Thus, $\Delta_1(L_A > \xi) = \Delta_1(\xi)$ should saturate, which is indeed seen for higher values of W and U for which ξ becomes shorter. Another feature of $\Delta_1(L_A)$ which should be considered is its magnitude. A simple consideration, treating the fact that the entanglement is confined to the boundary between the regions as an effective confining potential of width ξ in H_A (see Fig 1), will result in $\Delta_1(\xi) \propto 1/\xi$. This argument neglects the fact that we are calculating the level spacing within the same sector N_A . Thus one must consider that the next state might not belong to the same N_A sector. Taking into account that the variance in the number of particles in region A is proportional to $\sqrt{\xi}$ one concludes that $\Delta_1(\xi) \propto 1/\sqrt{\xi}$.

This behavior is seen in Fig. 3 where Δ_1 for different values of disorder and interaction are indicated by the symbols. Since (except for $W = 0.3$) in all cases $\xi \leq 200$ we have also averaged over the different values of L_A in the range $L/4 < L_A < 3L_A/4$, where the first level spacing saturates. In the top figure, Δ_1 is plotted as function of $1/\sqrt{\xi_0} \propto W$. As indicated by the black line, for the non-interacting case ($U = 0$) as long as $\xi < L$ (i.e., $W > 0.4$) the numerical data follows $1/\sqrt{\xi_0}$ perfectly. For the interacting cases, deviations are clearly seen. That is not surprising since ξ depends on U . Taking the dependence of the localization length on the interactions into account by $1/\sqrt{\xi} \propto W^{1/(3-2K(U))}$ a linear relation of the form $\Delta_1 = \Delta_0(U)/\sqrt{\xi} + \text{Const}$ can be seen in the lower panel of Fig. 3. Moreover as can be seen in the inset $\Delta_0(U)$ depends linearly on U as may be expected from the level spacing of charged particles in a confined po-

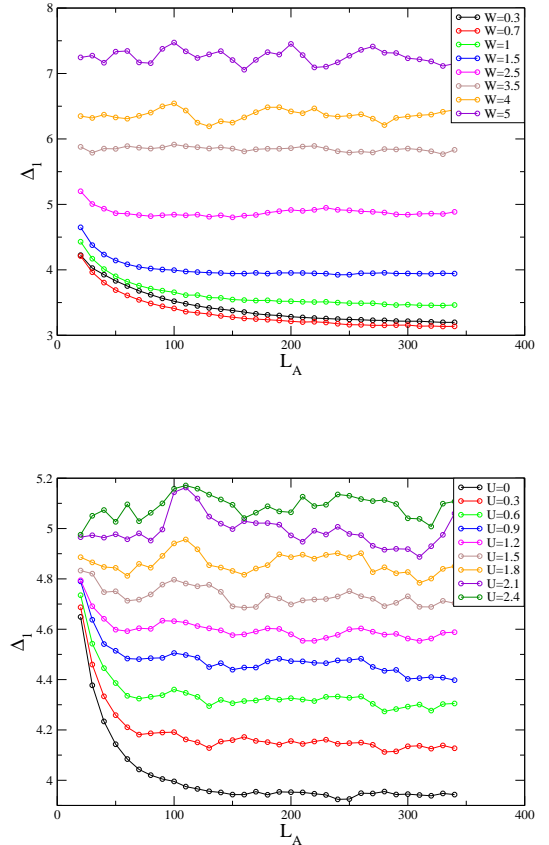


FIG. 2: The averaged first level spacing Δ_1 as function of the size of region A, L_A for a system of size $L = 700$ and different values of disorder W or interaction strength U . Top: The non-interacting case for different values of W . Bottom: For $W = 1.5$ ($\xi_0 = 50$) and different values of U . In both cases it is clear that as ξ decreases whether due to increasing disorder or interaction strength, Δ_1 saturates at smaller values of L_A , indicating a finite region in A influenced by the entanglement.

tential (Coulomb blockade)²¹. This further strengthens the picture of the entanglement spectrum corresponding to a many-particle spectrum of an effective Hamiltonian with a confining potential near the boundary.

Up to now we have considered the case for which the pure state $|\Psi\rangle$ of the entire system is the ground state. Of course, in principle one may calculate the entanglement spectrum of the system for any pure state. Nevertheless, DMRG is suitable only for the calculation of low-lying excitations, and therefore here we have calculated only the entanglement spectrum for these states. In the strong disorder regime, no physical difference is expected between the ground state and the low-lying excitations. Indeed, comparing Δ_1 for the ground-state and the first excited state for $U = 1.8, W = 2.5$ (Fig. 4), no significant difference can be seen. On the other hand, for weak disorder it has been shown that even for low-

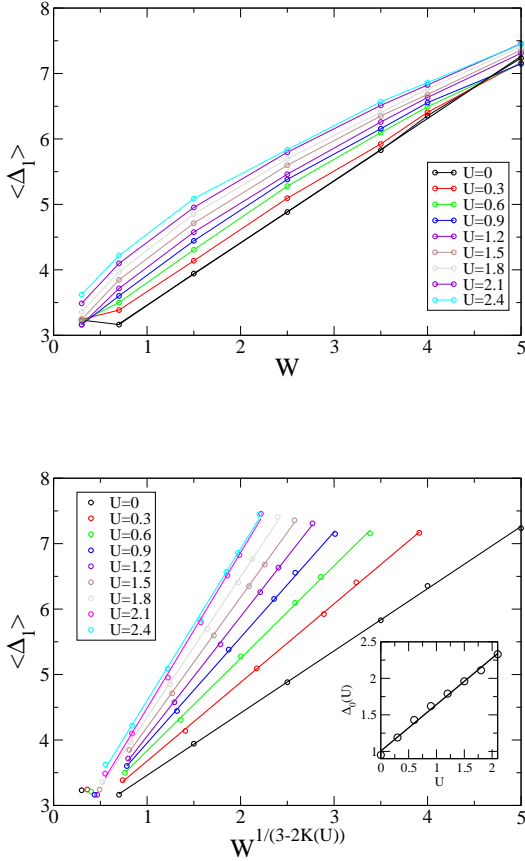


FIG. 3: The averaged first level spacing Δ_1 as function of the disorder W and interaction strength U averaged also over the central region on the wire $L/4 < L_A < 3L_A/4$ (symbols). Top: Δ_1 as function of the disorder strength. For the non-interacting case ($U = 0$) as long as $\xi < L$ (i.e., as long as $W > 0.5$) Δ_1 is linearly dependent on W (black line), in line with the expectation from $\Delta_1 \propto 1/\sqrt{\xi_0}$. This relation does not hold for the interacting case $U > 0$. Bottom: Taking into account the influence of U on the localization length. Here we plot Δ_1 as function of $1/\sqrt{\xi} \propto W^{1/(3-2K(U))}$. A linear dependence on $1/\sqrt{\xi}$ with a slope depending on interaction $\Delta_0(U)$ is clear (lines). As expected from interacting particles in a confining potential $\Delta_0(U) \propto U$ as can be seen in the inset

lying excitations there may be a significant increase in the localization length¹². This can be seen for the weak disorder case of $U = 0.6, W = 0.7$, as a decrease in Δ_1 for the saturated area, as expected when ξ increases.

IV. FIRST ENTANGLEMENT LEVEL SPACING DISTRIBUTION

One might naively expect that the distribution of the first entanglement level spacing will be similar to the first excitation of a localized many-particle system, which should follow the single-particle level spacing dis-

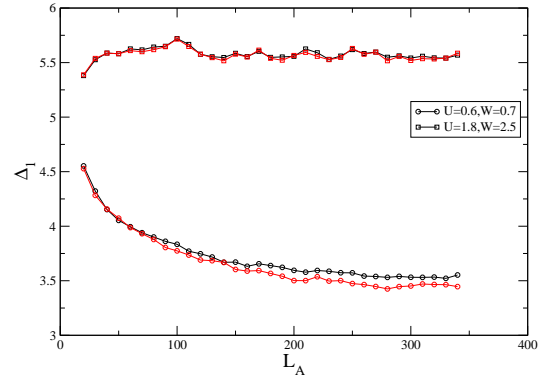


FIG. 4: Comparison of the averaged first entanglement level spacing between the ground-state (black) and the first excited state (red). For the strongly localized case $U = 1.8, W = 2.5$ there is no difference between the two. On the other hand, for the weak disorder case, $U = 0.6, W = 0.7$, Δ_1 is consistently lower in the saturated region for the excited state.

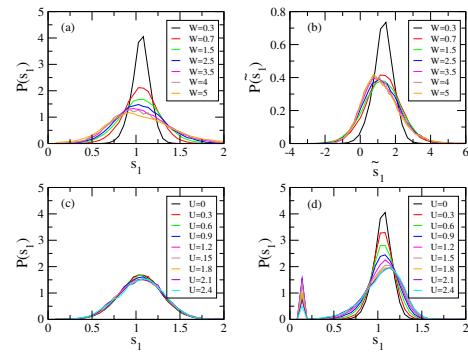


FIG. 5: The numerical distribution of the normalized first entanglement level spacing s_1 for different strength of disorder W and interaction strength U . (a) The distribution for different strength of disorder in the non-interacting ($U = 0$) case. (b) As in (a) where s_1 is rescaled according to $\tilde{s}_1 = (s_1 - 1) * (a + bW) + 1$ and $P(\tilde{s}_1) = (a + bW)^{-1}$ where a and b are constants. (c) The distribution for different strength of interaction strength at a given value of disorder $W = 1.5$, the distribution is almost independent of U . (d) As in (c) for weaker disorder $W = 0.7$. In this case as U increases a second peak in the distribution for small spacings appears.

tribution, i.e., the Poisson distribution²². The distribution of the normalized first excitation $P(s_1)$ (where $s_1 = (\varepsilon_2^{N_A} - \varepsilon_1^{N_A})/\Delta_1^{N_A}$) is drawn from different realization of disorder, different cuts of L_A in the range $L/4 < L_A < 3L/4$ and values of $N_A \sim L_A/2$ and presented in Fig. 5(a) for the non-interacting ($U = 0$) case. It is immediate clear that this is not a Poisson distribution, but rather a Gaussian-like broadening of the spacing

as function of W . This non-universal behavior of the distribution is due to the effective confining potential of the entanglement Hamiltonian. Since only an area of length ξ is sampled by the entanglement spectrum the system on this length scale is not localized. As is known for disordered 1D systems the distribution of single-particle level spacing crosses over very rapidly from a universal Poisson distribution when ξ is smaller than the length to a non universal broadening as ξ becomes larger than the systems length, with no true Wigner behavior in the middle²³. Thus $P(s_1)$ shows the typical behavior of a short disordered 1D system. The broadening of the distribution is proportional to W , and the distribution might be rescaled by $\tilde{s}_1 = (s_1 - 1) * (a + bW) + 1$ and $P(\tilde{s}_1) = (a + bW)^{-1}$ with the numerical factors $a = 0.17$, $b = 0.0375$. As can be seen in 5(b) after the rescaling the curves with stronger disorder ($W > 0.7$) for which the localization length is significantly shorter than the system size, all curves fall on each other.

In the region where $\xi \ll L$ there is no dependence on U as is demonstrated in 5(c) for the case of $W = 1.5$. Thus, in contrast with the average first level spacing which depends on ξ the distribution width depends only on the on-site disorder W and not on U or ξ . Nevertheless, for weak disorder ($W = 0.7$, $\xi \geq L$) a peculiar dependence on U appears. As is seen in 5(d) a second peak in the distribution at low values of s_1 appears. This peak has a non-monotonous behavior as function of U . It is absent for $U = 0$ increases as U increases up to $U = 1.2$ and then decreases. This feature is absent from stronger disordered samples (see, 5(c)).

V. INTERMEDIATE REGIONS IN WEAKLY DISORDERED STRONGLY INTERACTING REALIZATIONS

From where does this second peak for weakly disordered strongly interacting systems come from? Some insight may be gained from scrutinizing specific realizations of disorder. Four representative realizations with ($W = 0.7$, $U = 2.4$) are shown in Fig 6. For typical regions of each sample s_1 fluctuates around the average and are significantly higher than for a clean case with the same interaction strength ($W = 0$, $U = 2.4$). Nevertheless, there are rare regions (see, e.g., the lowest panel of Fig 6 in the region $370 < L_A < 470$) where s_1 is significantly lower than the average and much closer to the clean case value. Moreover, the entanglement entropy, S_A is strongly enhanced in that region even beyond the clean sample value. Likewise, the particle number variance $\delta^2 N_A = \langle N_A^2 \rangle - \langle N_A \rangle^2$ (easily calculated using DMRG), is also enhanced in this region, much beyond to the values for a clean system ($W = 0$) with the same interaction strength. The correspondence between S_A and $\delta^2 N_A$ seems to work well for these realizations although strictly speaking, there is no theoretical proof for this relation in interacting systems^{24–26}. This will

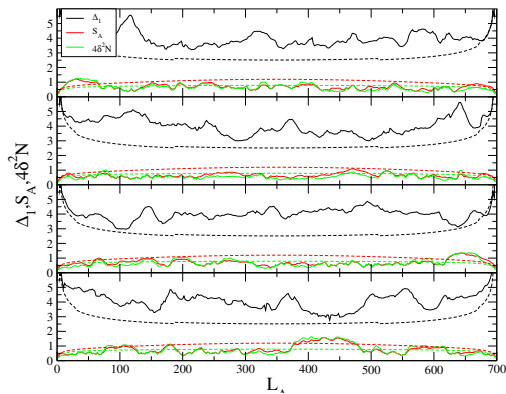


FIG. 6: The first entanglement level spacing s_1 (black curve), the entanglement entropy S_A (red curve), and the particle number variance $\delta^2 N_A$ (green curve multiplied by 4 for clarity) for four different realizations of disorder, where $W = 0.7$ and $U = 2.4$ and $L_A = 2, 4, 6, \dots, L - 2$. The results for a clean system ($W = 0$, $U = 2.4$) are presented by the corresponding dashed curves.

be further discussed elsewhere. Anyway, the behavior of both S_A and $\delta^2 N_A$ are in line with a “metallic” inclusion within the localized sample. Thus, although as we have seen for Δ_1 , on the average stronger interactions (U) corresponds to stronger localization (smaller ξ), there exist rare regions for which the interplay between interaction and disorder may lead to a more metallic-like behavior. A similar behavior, where interactions lead to delocalization in rare realizations of 1D disordered systems, was seen for the persistent current²⁷, and is also reminiscent of the intermediate microemulsion phases proposed for two-dimensional systems²⁸.

Some light on the nature of these rare regions can be shed by the low-lying entropy energies $\varepsilon_i^{N_A}$. Usually, for the half-filled case discussed here, and an even partition (L_A even), $\varepsilon_1^{N_A=L_A/2}$ is much lower than any other energy, since a state with $N_A = L_A/2$ is the most probable. Thus, one expects $\delta_1 = \min(\varepsilon\{N_A = L_A/2 \pm 1\}) - \varepsilon_1^{N_A=L_A/2}$ to be smaller than Δ_1 , but not orders of magnitude lower. Indeed, comparing δ_1 to Δ_1 for the last realization depicted in Fig. 6 (see Fig. 7) shows this behavior for most of the sample, except for the region around $370 < L_A < 470$, and smaller regions around $L_A = 100$ and $L_A = 600$ where δ_1 reaches values close to zero. These are exactly the regions where strongly enhanced values of S_A and $\delta^2 N_A$ are seen, i.e., close to the values of a metallic sample ($U = 0$, $W = 0$). For typical regions of the strongly interacting weakly disordered system the ground state is a pinned charge density wave leading to small variance in the number of particles and low entanglement entropy. In contrast, the rare regions are neither described by a charge density wave nor by a simple metallic behavior. This can be clearly seen from the very different behavior of δ_1 in these regions com-

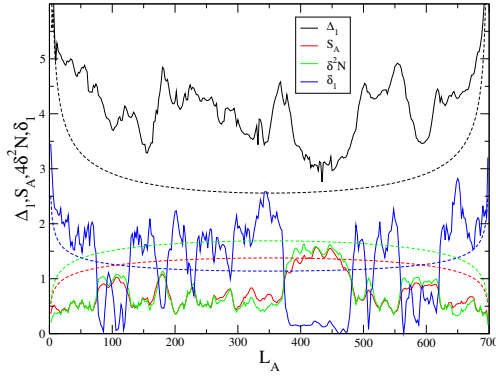


FIG. 7: A closer look at the behavior of the last realization depicted in Fig. 6. The first entanglement level spacing s_1 (black curve), the entanglement entropy S_A (red curve), the particle number variance $\delta^2 N_A$ (green curve multiplied by 4 for clarity) and the spacing between two lowest entropy levels belonging to different particle number, δ_1 (blue curve). For comparison the same variables calculated for a clean non-interacting sample ($U = 0$, $W = 0$) are indicated by dashed curves.

pared to regular metals. As seen in Fig. 7, especially for the region around $370 < L_A < 470$, δ_1 is much lower for the disordered rare region than for a clean system. This indicates that these rare regions are governed by different physics than the usual metallic 1D system. The fact that $\delta_1 \sim 1$ indicates large and almost equal contribution to the many-particle state from sectors with different number of particles in region A, which is very different than for the clean metallic situation.

VI. DISCUSSION

Thus, the average of the first entanglement level spacing has been shown to have a clear relation to the ground state localization length and shows the expected behavior as function of the strength of the on-site disorder

and with the repulsive particle-particle interactions. This stems from the fact that for a strongly localized system, the entanglement is confined to a distance of order of the localization length from the boundary between the regions, and that has a clear imprint on the low-lying eigenvalues of the RDM and the corresponding values of the entanglement Hamiltonian. The distribution of the first entanglement level spacing once the localization length is shorter than the sample length is Gaussian-like and quite universal. The distribution depends only on the strength of disorder and not on the interactions. Such a behavior is actually expected for the distribution of low-lying level spacings in a disordered confining potential, as long as the level spacing is larger than the influence of the disorder.

On the other hand, for weakly disordered systems and strongly interacting systems, the distribution shows an interesting peak, signifying an increased probability for almost degenerate level spacings. On closer examination of the behavior for specific realization it becomes clear this feature is connected to rare regions in the sample which exhibit metallic-like behavior. These rare regions in the ground state are composed of more or less equal significant contributions from two states with different number of particles. This not only leaves a distinct signature in the entanglement spectrum, but also leads to large variance in the number of particles in the region and high entanglement of the order of the values seen for free fermions. These intermediate microemulsion metallic phases embedded in an insulating phase. Further study of their properties is needed as well as their connection to the phase separation in two-dimensional systems²⁸, and to the enhancement of the persistent current in rare disordered systems²⁷.

Acknowledgments

Useful discussions with A. Turner and G. Murthy are gratefully acknowledged.

¹ P.W. Anderson, Phys. Rev., **109**, 1492 (1958).

² J.-y. Choi, S. Hild, J. Zeiher, P. Schauss, A. Rubio-Abadal, T. Yefsah, V. Khemani, D. A. Huse, I. Bloch, and C. Gross, Science **352**, 1547 (2016) and references therein.

³ R. Stano and P. Jacquod, Nature Photon. **7**, 66 (2013) and references therein.

⁴ For a review see: P. A. Lee and T. V. Ramakrishnan, Rev. Mod. Phys. **57**, 287 (1985).

⁵ R. Berkovits, Phys. Rev. Lett. **108**, 176803 (2012).

⁶ A. Zhao, R.-L. Chu, S.-Q. Shen, Phys. Rev. B **87**, 205140 (2013).

⁷ H. Li and F. D. M. Haldane, Phys. Rev. Lett. **101**, 010504 (2008).

⁸ N. Laflorencie, Phys. Rep. **646**, 1 (2016) and references therein.

⁹ M. Koch-Janusz, K. Dhochak, and E. Berg, Phys. Rev. B **95** 205110 (2017).

¹⁰ V. Alba, M. Haque, and A. M. Läuchli, Phys. Rev. Lett. **108**, 227201 (2012).

¹¹ M. Serbyn, A. A. Michailidis, D. A. Abanin, and Z. Papić, Phys. Rev. Lett. **117**, 160601 (2016).

¹² R. Berkovits, Phys. Rev. B **89** 205137 (2014).

¹³ R. A. Römer and M. Schreiber, Phys. Rev. Lett. **78**, 515 (1997).

¹⁴ F. Woynarovich and H. P. Eckle, J. Phys. A **20**, L97 (1987); C. J. Hamer, G. R. W. Quispel, and M. T. Batchelor, ibid.

- 20**, 5677 (1987).
- ¹⁵ T. Giamarchi, *Quantum Physics in One Dimension* (Oxford University Press, New York, 2003).
 - ¹⁶ W. Apel, J. Phys. C **15**, 1973 (1982); W. Apel and T. M. Rice, Phys. Rev. B **26**, 7063 (1982).
 - ¹⁷ T. Giamarchi and H. J. Schulz, Phys. Rev. B **37**, 325 (1988).
 - ¹⁸ S. R. White, Phys. Rev. Lett. **69**, 2863 (1992); Phys. Rev. B **48**, 10345 (1993).
 - ¹⁹ U. Schollwöck, Rev. Mod. Phys. **77**, 259 (2005); K. A. Hallberg, Adv. Phys. **55**, 477 (2006).
 - ²⁰ H. F. Song, S. Rachel, C. Flindt, I. Klich, N. Laflorencie, and K. Le Hur, Phys. Rev. B **85**, 035409 (2012).
 - ²¹ D.V. Averin and K.K. Likharev, J. Low Temp. Phys. **62**, 345, (1986).
 - ²² R. Berkovits, Europhys. Lett. **25**, 681 (1994); R. Berkovits and Y. Avishai, J. of Phys. Condens. Matter **8**, 389 (1996); R. Berkovits and B. I. Shklovskii, J. Phys. Condens. Matter **11**, 779 (1999).
 - ²³ A. Wobst, G.-L. Ingold, P. Hänggi, and D. Weinmann Eur. Phys. J. B **27**, 11 (2002),
 - ²⁴ I. Klich and L. Levitov, Phys. Rev. Lett. **102**, 100502 (2009).
 - ²⁵ B. Hsu, E. Grosfeld, and E. Fradkin, Phys. Rev. B **80**, 235412 (2009).
 - ²⁶ H. F. Song, S. Rachel, C. Flindt, I. Klich, N. Laflorencie, and K. Le Hur, Phys. Rev. B **85**, 035409 (2012).
 - ²⁷ P. Schmitteckert, R. A. Jalabert, D. Weinmann, and J.-L. Pichard, Phys. Rev. Lett. **81**, 2308 (1998).
 - ²⁸ B. Spivak and S. A. Kivelson, Phys. Rev. B **70**, 155114 (2004); R. Jamei, S. Kivelson, and B. Spivak, Phys. Rev. Lett. **94**, 056805 (2005).